Available online at www.sciencedirect.com
ScienceDirect
Polymer 48 (2007) 3961–3973
polymer
www.elsevier.com/locate/polymer

Direct fluorination of various poly(*p*-phenylene): Effects of the polymer synthesis and thermal post-treatment

Wei Zhang, Marc Dubois*, Katia Guérin, André Hamwi

Laboratoire des Matériaux Inorganiques, UMR CNRS-6002, Université Blaise Pascal Clermont-Ferrand, 63177 Aubière, France

Received 23 February 2007; received in revised form 27 April 2007; accepted 2 May 2007
Available online 7 May 2007

Abstract

In order to complete a preliminary work about the direct fluorination of poly(*p*-phenylene) (PPP), the main parameters of the process were investigated. The molecular (chain length and crystallinity) and morphological effects (B.E.T. surface, granulometry) were studied. So, two new starting samples were studied in addition to PPP synthesized by the Kovacic's method (i) a commercial PPP (Polysciences) and (ii) a pyrolyzed PPP, which is similar to an amorphous hydrogenated carbon. Moreover, an annealed PPP (Kovacic's synthesis and post-treatment at 400 °C for 36 h) was compared to the as-synthesized polymer. The reactions with F_2 gas differ significantly in accordance with the synthesis way and the post-treatment (annealing or pyrolysis). Investigations about the direct fluorination of PPPs were carried out for a better understanding of their behavior with respect to molecular fluorine. An extensive characterization was performed by complementary techniques (^{19}F and ^{13}C NMR, FT-IR, and EPR). The fluorine content in the fluorinated PPPs is evaluated by these methods and a reaction mechanism is proposed.

Keywords: Fluorinated polymer; Poly(*p*-phenylene); Fluorination

1. Introduction

Fluorinated polymers exhibit many desirable physicochemical properties, such as high thermal and chemical stabilities, hydrophobicity, optical transmittance, *i.e.* transparency in visible and UV, good friction coefficient, gas separation properties, low surface energy when compared to their non-fluorinated analogs and wettability [1–3]. So, their application range is large, including the uses as electrolyte membrane in fuel cell system, as membrane for gas separation, as membrane and separation for chloro alkali cell and batteries, as coatings and containers for handling aggressive products due to their exceptional thermal stability, chemical resistance and dielectric properties, as catalyst support for use under severe reaction conditions due to the improvement in thermal stability and hydrophobicity [4].

Two distinct ways of synthesis can be used: (i) polymerization of fluorine containing monomers (*e.g.* tetrafluoroethylene to obtain polytetrafluoroethylene) as for many commercial fluoropolymers; (ii) incorporation of fluorine atoms into a non-fluorinated parent polymer. The first method requires the availability of reactive fluorinated monomers, excluding in some cases, this way. Fluorination becomes thus a good alternative way to modify the polymer and to form new fluorinated materials with tuneable properties as a function of the fluorine content. So, the high reactivity of fluorine can be favourably used to modify and/or to protect the surface of the commercial polymers [1,2]. The fluorination process can be limited to the surface using low treatment duration, low fluorine partial pressure, low fluorination temperature or by the use of fluorinating agents. But, to our opinion, for the complete understanding of the process, fluorination must be extended toward the grain core. This is the choice that we did in the case of poly(*p*-phenylene) by the use of pure fluorine gas.

In relation to their applications, direct fluorination of polymers was successfully used to reduce the refractive index [5],

* Corresponding author. Tel.: +33 4 73 40 71 05; fax: +33 4 73 40 71 08.
E-mail address: marc.dubois@univ-bpclermont.fr (M. Dubois).

0032-3861/$ - see front matter © 2007 Elsevier Ltd. All rights reserved.
doi:10.1016/j.polymer.2007.05.001

the friction coefficient [6], to improve their optical transparency and their hydrophobicity to render the surface impermeable to the hydrocarbon fuels [1], and to modify wettability [7]. Many commercial polymers were fluorinated by this way: polyethylene, polypropylene, polystyrene, sulfonated polystyrene, poly(ethylene terephthalate), polyamide and so on [7–9].

The goal of the present work is to study fluorination of a linear π-electron conjugated system since the electronic properties of such systems have a great interest. A conjugated polymer, poly(*p*-phenylene) abbreviated as PPP, was then used as starting material for fluorination. It consists of phenyl rings linked exclusively in *para* position. This polymer exhibits good chemical and thermal stabilities, up to 500 °C, due to π-delocalization along the polymer chain.

In addition to our preliminary study of the fluorination of Kovacic PPP, in which the reactivity of the polymer with fluorine gas was discussed [6], this paper focuses on the parameters involved in the fluorination mechanism. The molecular (chain length and crystallinity) and morphological effects (B.E.T. surface, granulometry) were investigated.

For this goal, three different kinds of poly(*p*-phenylene) were fluorinated. Amongst the various synthesis of PPP, chemical [10–14] or electrochemical [15], the chemical Kovacic's method [13,14] was chosen to prepare a polymer with longer chain than the other synthesis [14] for which the main characteristics can be evaluated (crystallinity, chain length, surface area). In addition, a commercial PPP produced by Polysciences, as well as the product of the partial pyrolysis of this one, has been also investigated. The comparison of the reactivities of the polymers resulting from three different preparation modes allows the effect of fluorination on the characteristics of each product such as the granulometry, the chain length, the various H/C molar ratios resulting from a thermal treatment (annealing or pyrolysis), and the presence of oligomers to be determined.

The materials obtained were characterized by various techniques such as Fourier Transform Infrared (FT-IR) spectroscopy and high resolution solid state Nuclear Magnetic Resonance (NMR) (^{19}F, ^{13}C) which are adapted to determine the nature of the C–F bonding and the fluorinated groups (CF, CF_2, CF_3…). Electron Paramagnetic Resonance (EPR) allows investigating the connection defects which are created during fluorination. X-ray diffraction (XRD), specific surface measurement (B.E.T.), Laser Granulometry and Scanning Electron Microscopy (SEM) supplement this characterization. Moreover, a careful investigation of the starting material by these methods is necessary to understand the fluorination mechanism.

2. Experimental

2.1. Synthesis and fluorination

The most current PPP synthesis is that initiated by Kovacic [13,14] which consists in polymerization of benzene in the presence of a catalyst, aluminum chloride ($AlCl_3$), and an oxidant, cuprous chloride ($CuCl_2$). The obtained powder exhibits a brown color; it is denoted as PPP_K. Its chemical composition is $C_6H_{3.85}$, *i.e.* 92.2% (weight/weight) of C, 4.9% of H, a low amount of catalytic residues is also present (~1.1% Cl, 0.4% Al, 0.1% Cu). The chemical composition of $C_6H_{3.85}$ instead of the theoretical C_6H_4 is explained by the presence, in low amounts, of other connection modes than *para* along the chains, of cross-linking, and of residual chlorine at the chain endings [14,16].

The sample was annealed under dynamic vacuum at 400 °C for 36 h in order to improve both the crystallinity and the chain length. Other parameters change during this process and will be discussed later. The annealed polymer is called PPP_K-T400. The chemical composition slightly changes after annealing: $C_6H_{3.81}$. PPP provided by Polysciences exhibits yellow colour. It is denoted as PPP_P, with a chemical composition of $C_6H_{2.88}$. Because it contains phenylene oligomers [17], a treatment at 250 °C for 12 h under vacuum was applied to remove most of these species (denoted as PPP_P-T250). All the samples are synthesized as insoluble powders.

Fluorination was carried out under a pure fluorine gas flow (14 ml/min) at room temperature; the fluorine pressure is equal to the ambient pressure. Fluorine gas (Solvay FLUOR GmbH) contains traces of oxygen. So, the formation of C=O containing groups (*e.g.* –C(=O)F) in the fluorinated PPP did not occur. Each sample (about 0.1 g) was placed in a Monel boat. The chemical compositions are given in Table 1 as a function of the fluorination duration (0.33, 1, 2, 14 and 24 h); these values were obtained by weight uptake assuming that the linking of one fluorine atom results in an increase of 18 g per mol when x in C_6F_x is lower than 4 (substitution of hydrogen by fluorine) and of 19 g per mol for $x > 4$ (fluorine addition). These data display the fluorination level rather than the chemical composition, which must be given as $C_6F_xH_y$. This parameter was chosen to compare the samples which exhibit various hydrogen contents in the virgin state.

2.2. Physicochemical characterization

NMR experiments were performed with Bruker Avance spectrometer, with working frequencies for ^{13}C and ^{19}F of 73.4 and 282.2 MHz, respectively. A Magic Angle Spinning probe (Bruker) operating with a 4 mm rotor was used. For MAS spectra, a simple sequence (τ-acquisition) was performed with a single π/2 pulse length of 4 and 3.5 μs for ^{19}F and ^{13}C, respectively. ^{13}C chemical shifts were externally referenced to tetramethylsilane (TMS). ^{19}F chemical shifts were referenced with respect to $CFCl_3$.

Table 1
Fluorination level, *i.e.* x in C_6F_x for various fluorination duration

Starting polymer	Fluorination duration (h)				
	0.33	1	2	14	24
PPP_K	$C_6F_{7.3}$	$C_6F_{7.7}$	$C_6F_{8.4}$	$C_6F_{7.8}$	–
PPP_P	$C_6F_{2.4}$	$C_6F_{3.1}$	$C_6F_{7.4}$	$C_6F_{7.8}$	–
PPP_P-T250		$C_6F_{0.4}$	$C_6F_{1.5}$	$C_6F_{4.2}$	$C_6F_{5.2}$

EPR spectra were performed with a Bruker EMX digital X band ($\nu = 9.653$ GHz) spectrometer. Diphenylpicrylhydrazyl (DPPH) was used as the calibration reference to determine both the resonance frequency and the densities of spin carriers.

Powder X-ray Diffraction (XRD) measurements were carried out using a Siemens D501 diffractometer working with a Cu(K_α) radiation. Fourier Transform Infrared (FT-IR) spectroscopy was performed using spectrometer THERMO NICOLET 5700; the spectra were recorded by transmission in a dry air atmosphere between 400 and 4000 cm^{-1} with 64 spectral accumulations.

Thermogravimetric analysis (TGA) was carried out with about 20 mg of product under a dry argon atmosphere. A heating rate of 2 °C min^{-1} was used.

The textural characterization of the samples was performed on a Quantachrome Autosorb gas sorption system. The instrument permits a volumetric determination of the isotherms by a discontinuous static method at 77.4 K. The adsorptive gas was nitrogen with a purity of 99.999%. The surface area was obtained to the N_2 isotherm. The cross-sectional area of the adsorbate was taken to be 0.162 nm^2 for specific surface area (SSA) calculation purposes. Prior to N_2 sorption, all samples were degassed at 120 °C for 12 h under reduced pressure. The masses of the degassed samples were used in order to estimate the SSA which was determined by applying the B.E.T. method and taking at least 5 points in the $0.05 < P/P_0 < 0.3$ relative pressure range.

The microstructural characteristics were checked by Scanning Electron Microscopy (SEM) on a Cambridge Scan 360 operated at 10 kV as well as by Laser Granulometry (Mastersizer, from Malvern Instruments). For these light scattering experiments, the samples were dispersed in water with ultrasounds. A polydisperse model was used for calculations and the residual was ensured to be less than 1% for all measurements.

Particle-size distributions in the size range 0.04–900 μm were calculated from the diffraction data using the Fraunhofer model. Several statistical parameters were derived from the primary data, including average diameter and diameter distribution limits, which are defined as $D(v,0.1)$ (10th volumic percentile of the distribution) and $D(v,0.9)$ (90th percentile of the distribution).

3. Results

3.1. Fluorination level evolution and thermal stability

As expected, for the shorter fluorination durations, the higher the fluorination time is, the higher the fluorine level is (Fig. 1 and Table 1). After 20 min, fluorination of PPP_K results in a fluorination level of $C_6F_{7.3}$, meaning that the reactivity of this polymer is extremely high. At similar fluorination duration, the fluorine content varies for the various kinds of polymers. Such high fluorine contents, higher than the number of hydrogen atoms before the reaction, indicate a breaking of the aromatic character and a change of the carbon hybridization from sp^2 to sp^3. The reactivity with respect to fluorine

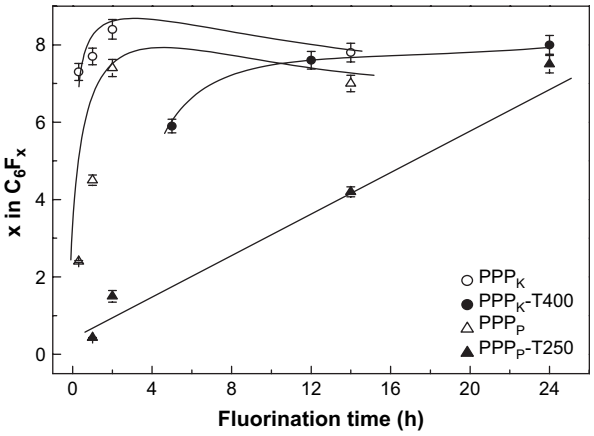

Fig. 1. Fluorination level as a function of the fluorination durations. Data concerning PPP_K-T400 [6] are added for comparison.

is higher for PPP_K and PPP_P compared to PPP_p-T250. More surprisingly, the mass uptake shows that the fluorination level decreases for both PPP_K and PPP_P when the fluorination time exceeds 12 h. This phenomenon can be explained by the fact that a prolonged fluorination is able to break the phenyl rings and then to form volatile alkyl fluorides such as CF_4, C_2F_6…; this decreases the total carbon mass and results in an underestimated value of x in C_6F_x.

Regarding the fluorine levels, the following classification can be established for the reactivity with F_2 gas: PPP_K strongly reacts; PPP_P is slightly less reactive whereas PPP_P-T250 thermally treated requires more time to reach high fluorine content. So, the fluorine content of PPP_P-T250 is still lower than that for the other polymers even for 24 h fluorination. In the following part, these differences will be explained by comparing the physicochemical properties of the various starting materials.

In order to check the chemical stability of the fluorinated samples, TGA was carried out (Fig. 2 and Table 2). As exemplified by PPP_K fluorinated for 0.33 h (Fig. 2b), a weight loss occurs during three temperature ranges, denoted as I, II and III. The first process (about 7–8%) is related to the desorption of moisture and/or HF molecules from the powder surface. During the second step, a good accordance is found between the theoretical weight losses, which are calculated assuming a total removal of the fluorine atoms starting from the C_6F_x chemical composition, and the experimental value (Table 2). This suggests that the main process during part II consists in a massive de-fluorination of the samples. The de-fluorination temperatures are extracted from the derivative TGA curve and reported in Table 2. It must be noted that, in accordance with its high chemical stability, the pristine PPP_K exhibits only 17% weight loss, occurring mainly in the 400–500 °C range. The amorphous carbons, which are formed by this de-fluorination, and/or residual non-fluorinated polymer are decomposed in the third step, resulting in a quasi-total disappearance of the sample (except PPP_P-T250 and PPP_P fluorinated for 2 and 0.33 h, respectively, the fluorine content being lower than that for the other samples).

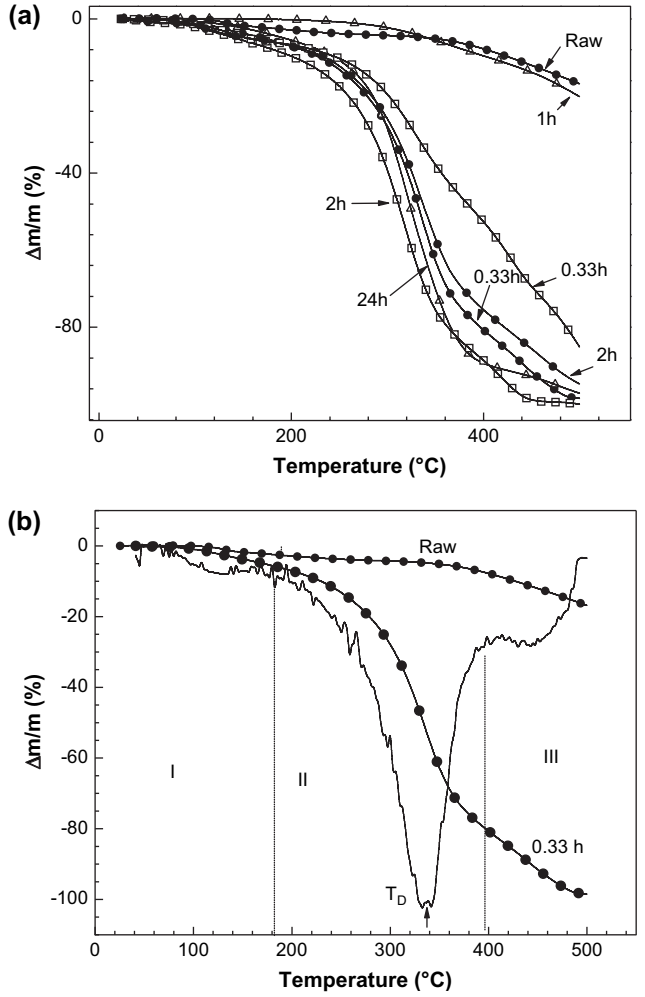

Fig. 2. TGA curves of various fluorinated samples; (●) PPP_K, (□) PPP_P and (△) PPP_P-T250 (a) and TGA and derivative curves of raw Kovacic PPP raw and fluorinated for 0.33 h (b). The decomposition temperatures T_D are reported in Table 2.

3.2. Physicochemical characterizations

First, it must be noted that, whatever the synthesis and the thermal treatment, the crystallinity of the polymer (about 30%) disappeared for the lower fluorination duration as revealed by X-ray diffraction (not shown here).

3.2.1. FT-IR spectroscopy

Fig. 3 shows the FT-IR spectra of the original and fluorinated PPP_K. After 20 min of fluorination at room temperature, a disappearance of the vibration modes of PPP is noted in the range 698–860 cm^{-1}; these lines are characteristic of the C–C or C–H vibration modes of mono- or parasubstituted phenyl rings (Table 3) [14]. This is accompanied by the simultaneous appearance of a strong band at 1200 cm^{-1}, assigned to covalent C–F bonds, and confirms the conversion of the C–H bonds into C–F ones. The broadness of the line at 1200 cm^{-1} results from a superimposition of several contributions: CF_3, CF_2, CHF, and CF.

As indicated by the chemical compositions (Table 1), FT-IR spectroscopy reveals that the connection modes of the phenyl groups differ in these two polymers (Fig. 3). The most intense modes in the range 650–1000 cm^{-1} are the C–C vibrations between the phenyl rings and the monosubstituted phenyls. PPP_P exhibits a weak para line and a strong intensity of the monosubstituted phenyls (698 and 764 cm^{-1}). Moreover, the *para* C–C vibration for PPP shifts toward the low wave numbers when the number of phenyl groups forming the chain increases revealing the presence of oligomers. This occurs for Polysciences PPP; the number of vibration bands also reveals the presence of oligomeric species, as reported in the literature [17]. Moreover, as in the case of the PPP_K, a similar process occurs with the appearance of the broad band at 1200 cm^{-1} related to the covalent C–F bond formation after fluorination. Contrary to the PPP_K, the intensity of this peak gradually grows with the fluorination duration in accordance with the evolution of the fluorination level. Less quickly for PPP_P than for PPP_K, the fluorine level increases as a function of the duration. In addition, this progressiveness of the fluorination in the case of the Polysciences PPP is also in accordance with the intensity of the vibration bands of the virgin polymer: a progressive decrease in the intensities of these bands is noticed. Two hours of fluorination are necessary for the total disappearance of these modes; the chemical formula of this compound is $C_6F_{7.4}$, such a fluorination level was obtained after 20 min for PPP_K.

The band at 850 and 980 cm^{-1}, which is assigned to CF_3 groups according to the works of Legeay et al. [18] and Lunkwitz et al. [19], indicates the breaking of some phenyl rings and then the formation of fluorinated side chains (*e.g.* CF_2–CF_3).

Table 2
TGA data of various fluorinated PPPs

Sample	Fluorination time (h)	Composition	Decomposition temperature T_D[a] (°C)	Weight loss in range II	Weight loss at 500 °C (%)
PPP_K	0.33	$C_6F_{7.3}$	337	66% (th.[b]), 71% (392 °C)	98
	2	$C_6F_{8.4}$	330	69% (th.), 69% (403 °C)	95
PPP_P	0.33	$C_6F_{2.4}$	330	39% (th.), 38% (372 °C)	85
	2	$C_6F_{7.4}$	316	66% (th.), 75% (381 °C)	99
PPP_P-T250	2	$C_6F_{0.4}$	333	10% (th.), 6% (354 °C)	20
	24	$C_6F_{5.2}$	316	58% (th.), 85% (418 °C)	97

[a] Extracted from derivative TGA curve.
[b] Theoretical weight loss considering that the fluorine atoms are totally removed.

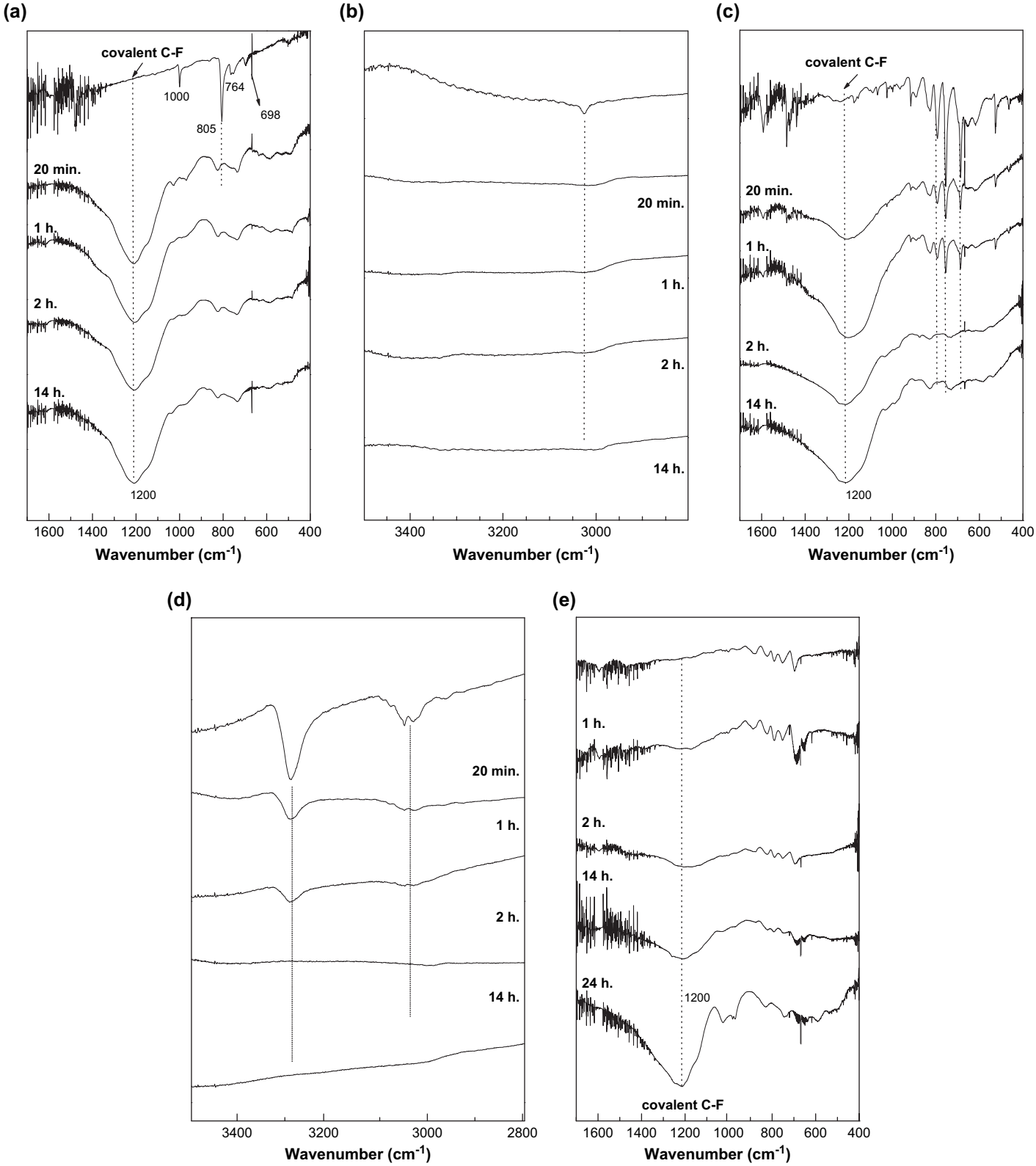

Fig. 3. FT-IR spectra of the virgin and fluorinated PPPs as a function of the treatment duration: PPP_K (a) and (b), PPP_P (c) and (d), and PPP_P-T250 (e).

The content of the C–H bonds, which exhibit vibration modes near 3000 cm^{-1}, decreases during the fluorination, even for the shortest durations for PPP_K, and more progressively for PPP_P (Fig. 3b and d). This wavenumbers range is not shown for PPP_P-T250 because any peak does not appear.

By comparing FT-IR spectra of PPP_P and PPP_P-T250, the lower intensities of the vibration bands from 800 to

Table 3
Assignment of the IR vibration modes of poly(*p*-phenylene)

PPP	Wave numbers (cm^{-1})	Vibration mode
Pristine	698	Out-of-plane C–H vibration (δ_{C-H}) of monosubstituted phenyl rings
	764	Out-of-plane C–H vibration (δ_{C-H}) of monosubstituted phenyl rings
	805	Out-of-plane C–C vibration (δ_{C-C}) of parasubstituted phenyl rings
	860	Out-of-plane C–H vibration (δ_{C-H}) of an isolated hydrogen
	1000, 1480 and 1398	In-plane C–C vibration (υ_{C-C}) of parasubstituted phenyl rings
	~3000	C–H vibration of aromatic rings (υ_{C-H})
	1800	C=C stretch
	~1200	Vibration of covalent C–F bonds (C–F, CF_2 or CF_3)
Fluorinated	980	CF_3 side groups
	850	CF_3 side groups
	730	CF_3 and CF_2 symmetric deformation

600 cm^{-1} for PPP_P-T250 indicate that the thermal treatment of PPP_P results in the elimination of the oligomers. Moreover, a hydrogen loss seems to occur as evidenced by the decrease and the shift of the C–H vibration modes. By analogy with the pyrolysis of Kovacic poly(*p*-phenylene) [20], a reorganization of the phenyl rings and the formation of hydrogenated amorphous carbons can occur during the thermal treatment. So, this treatment could be assimilated to a partial pyrolysis of the polymer. This rearrangement strongly influences the reactivity of the resulting product which becomes less reactive compared to the two other PPPs; 24 h duration time is necessary for a high fluorination level.

3.2.2. NMR study

The ^{13}C NMR spectrum of the virgin PPP_K was recorded with magic angle spinning procedure operating with a spinning rate of 10 kHz, as for the other samples. The area ratio of the lines centered at +128 and +139 ppm/TMS allows the chain length to be evaluated. As a matter of fact, these lines are assigned to carbon atoms linked to hydrogen atoms (with area under the curve S_{C-H}) and carbon atoms which ensure the connection between the rings (S_{C-C}), *i.e.* non-hydrogenated, respectively [6,21]. A chain length of 11–12 was found for PPP_K using the method described in the literature [14].

By comparison with the ^{13}C NMR spectrum of the virgin PPP_K (Fig. 4a), the sample fluorinated for 20 min does not present any more the two peaks at +128 ppm (C–H) and +139 ppm (C–C). This disappearance is correlated with the high fluorination level obtained after 20 min. In addition, two peaks located at +84 and +104 ppm appear in the first step of the fluorination. According to the literature concerning the fluorinated carbons and more particularly graphite fluorides [22–24] and fluorinated polymers, the second peak at +104 ppm is characteristic

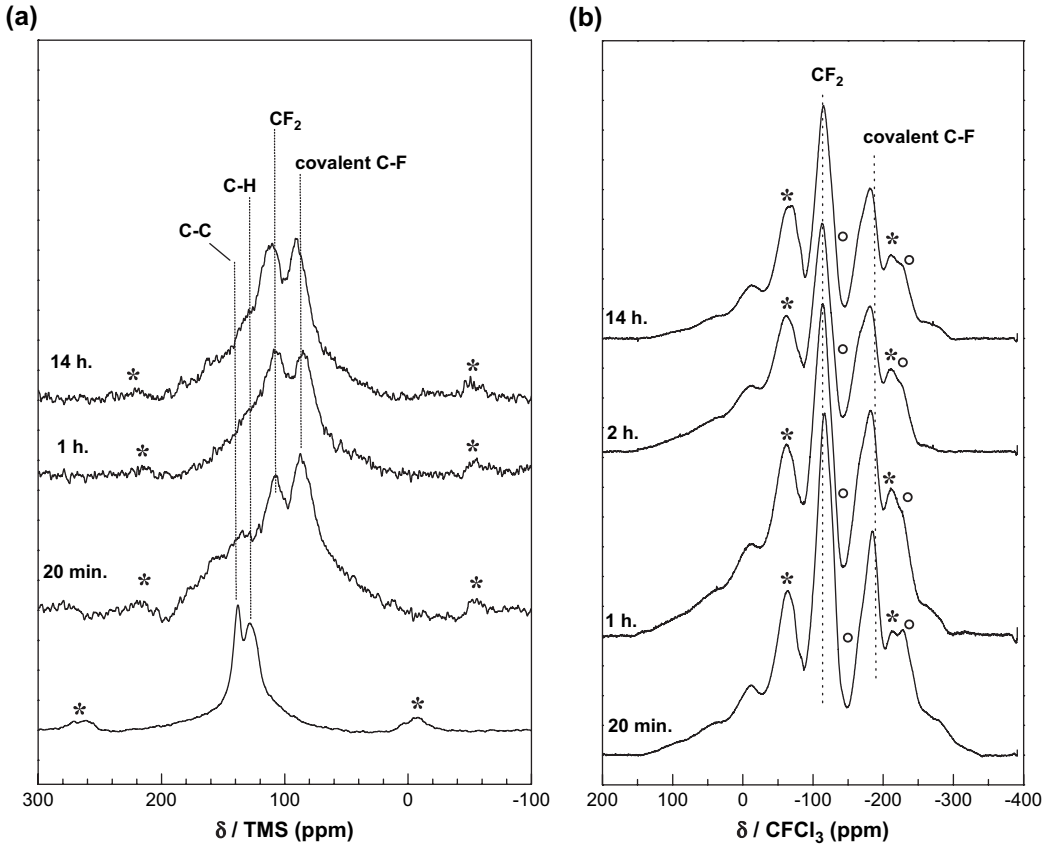

Fig. 4. ^{13}C (a) and ^{19}F MAS-NMR spectra (b) of the virgin poly(*p*-phenylene) and the fluorinated polymer as a function of the fluorination duration (the spinning rates are 10 and 14 kHz for ^{13}C and ^{19}F measurements, respectively). * and ° mark off the spinning sidebands.

of CF_2 groups along the polymeric chain. The carbon atoms involved in covalent C–F bonds in graphite fluoride exhibit a chemical shift ranged between +84 and +88 ppm, justifying the attribution of the peak at +84 ppm for the fluorinated PPP to this type of carbon atom in CF bonds. The relative proportion of the CF and CF_2 groups does not evolve during the fluorination. It is important to note that the ^{13}C chemical shifts for molecules CH_2F_2, CHF_3 and CF_4 are close: +111.2, +118.8, and +119.9 ppm, respectively. So, the broad peak centered at +110 ppm can be in fact an envelope containing the various contributions of $-CF_3$, $>CFH$, and $>CF_2$.

^{19}F NMR spectra of the fluorinated PPP_K (Fig. 4b) are close whatever the fluorination duration. Two distinct peaks, at −115 and −182 ppm/$CFCl_3$, are observed and correspond to CF_2 groups and the covalent C–F bonds, respectively. The broadness of the resonance line is due to strong $^{19}F-^{19}F$ homonuclear coupling. CF_3 groups are also present in the fluorinated PPPs as evidenced by a narrow line at −82.3 ppm. So, in accordance with FT-IR spectroscopy, these results confirm the loss of the aromatic character leading to CF_2 and the breaking of some phenyl rings, which forms CF_3 groups.

The ^{13}C NMR spectrum of the virgin PPP_P (Fig. 5a) reveals that in addition to the two peaks expected for the PPP chain (C–C and C–H) several peaks are present. The PPP_P is a commercial product and no post-treatment was applied in order to remove catalyst residues and non-polymerized monomers. So contrary to the PPP_K, the spectrum of the PPP_P presents three resonance lines and a shoulder at +124, +130, +133 and +143 ppm. This latter is assigned to C–C whereas the other peaks are related to protonated carbon atoms.

By combining FT-IR and NMR characterizations and in agreement with the assumptions of Brown et al. [17] who report the ^{13}C NMR spectra of the phenylene oligomers (from biphenylene to sexiphenylene), the presence of oligomers can be suspected. The line at +124 ppm is then attributed to protonated carbon atoms of these oligomers. Moreover, the NMR lines present in the range from +50 to +80 ppm are assigned to additional alkyl groups from the synthesis residues.

In comparison to PPP_K, PPP_P is less reactive with respect to fluorine gas. This result is confirmed by the conservation of the line at +143 ppm related to non-protonated carbon atoms (C–C). Another peak centered at +157 ppm is also visible; its intensity grows with the fluorination time. It is assigned to ^{13}C atoms in the aromatic rings (Φ) and interacting with the fluorine atoms (noted Φ-F) [6]. In the same way, the lines at +80 and +74 ppm disappear gradually when the fluorination time increases. So the reaction of fluorination starts with the elimination of the oligomers and/or the more reactive synthesis residues. This elimination can be carried out by the formation of perfluorinated compounds and their decomposition into volatile species (CF_4, C_2F_6…). The higher the π-delocalization is, *i.e.* the chain length, the higher the chemical stability of

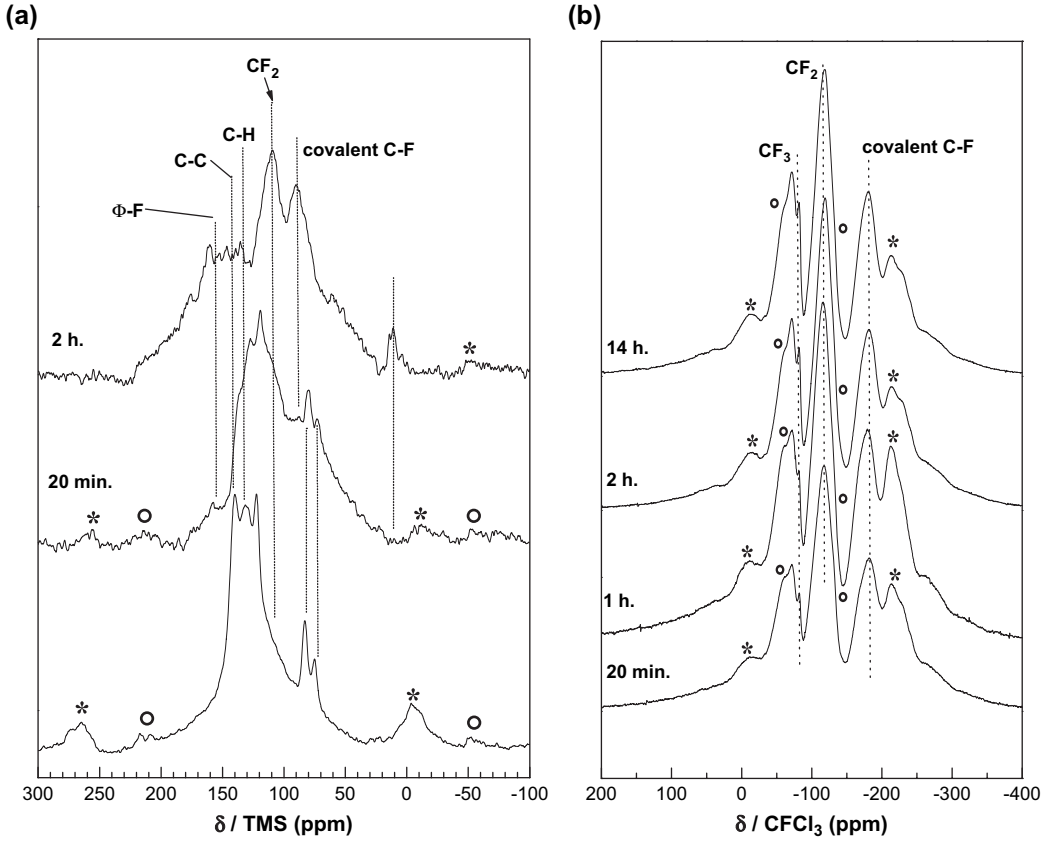

Fig. 5. ^{13}C (a) and ^{19}F MAS-NMR spectra (b) of the Polysciences poly(*p*-phenylene), as provided and fluorinated during various durations. * and ° mark off the spinning sidebands.

the polymer is. Then, the residual oligomers progressively react with F_2 forming volatile species, even at room temperature. Although this reaction is instantaneous, it progressively occurs because of the polymer grain size, as discussed later. Some monomers are trapped into the grain core and are then not accessible to F_2.

On the ^{19}F NMR spectra (Fig. 5b), the weak additional peak at −83.3 ppm, assigned to CF_3 groups, indicates their formation. Contrary to the other fluorinated groups, $-CF_3$ exhibits spinning molecular motion around the C−C bond which is responsible of the line narrowness. These CF_3 groups can be partly formed by the reaction of F_2 with the oligomers. This explains that they are clearly observed for the low fluorination duration. The lines at −119.5 and −180.5 ppm are related to fluorine in the CF_2 groups and in the CF bonds, respectively. As in the case of PPP_K, the CF_2/CF ratio does not significantly change for fluorination longer than 1 h.

The treatment of PPP_P at 250 °C during 12 h can be compared to a partial pyrolysis which consists in a removal of the not polymerized oligomers and in a hydrogen loss due to a reorganization of the phenyl rings to form hydrogenated amorphous carbons. The ^{13}C NMR of PPP_T-T250 (Fig. 6a) exhibits an intense peak at +138 ppm (C−C connection), whereas the line at +127 ppm assigned to the C−H is lower than that for PPP_P (Fig. 5a). As suggested before, small graphene sheets are formed by connection of several phenyl rings and hydrogen elimination during a process similar to a partial pyrolysis.

The reactivity of this treated PPP is appreciably attenuated in comparison with the initial polymer, since for the sample fluorinated for 2 h, the peaks characteristic of the C−F do not appear yet. Nevertheless, at approximately +84 (C−F) and +110 (CF_2) ppm, shoulders are present. After 14 h treatment, the fluorination of the pyrolyzed polymer is effective.

^{19}F NMR spectra in Fig. 6b present great similarities with the two other polymers. The resistance of this treated polymer with respect to molecular fluorine is sufficient to observe the intermediate step of the fluorination.

^{13}C NMR is more relevant to compare the fluorination of the various PPPs, making possible to underline the intermediate steps and the persistence of the polymer. With ^{19}F NMR, only qualitative information is provided whatever the duration since the same groups are formed during the fluorination, *i.e.* CF_2, C−F, and CF_3; only the area ratio of the various lines varies. The homonuclear coupling between ^{19}F nuclei results in a consequent widening of the lines, and thus the presence of numerous spinning sidebands in spite of a higher spinning speed ($\upsilon = 14$ kHz). Other techniques were then also performed to characterize the fluorinated carbons, such as EPR discussed in the following part.

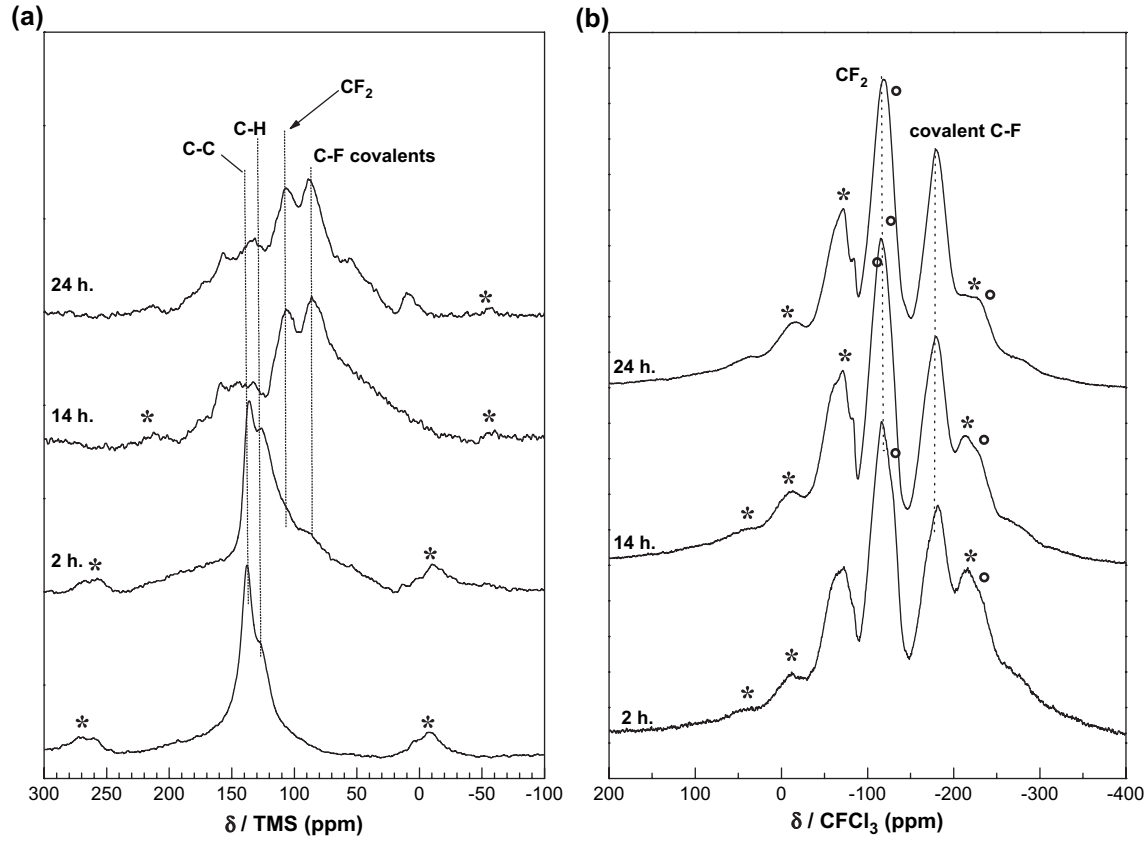

Fig. 6. ^{13}C (a) and ^{19}F MAS-NMR spectra (b) of commercial poly(*p*-phenylene) post-treated at 250 °C and fluorinated for various times. * and ° mark off the spinning sidebands.

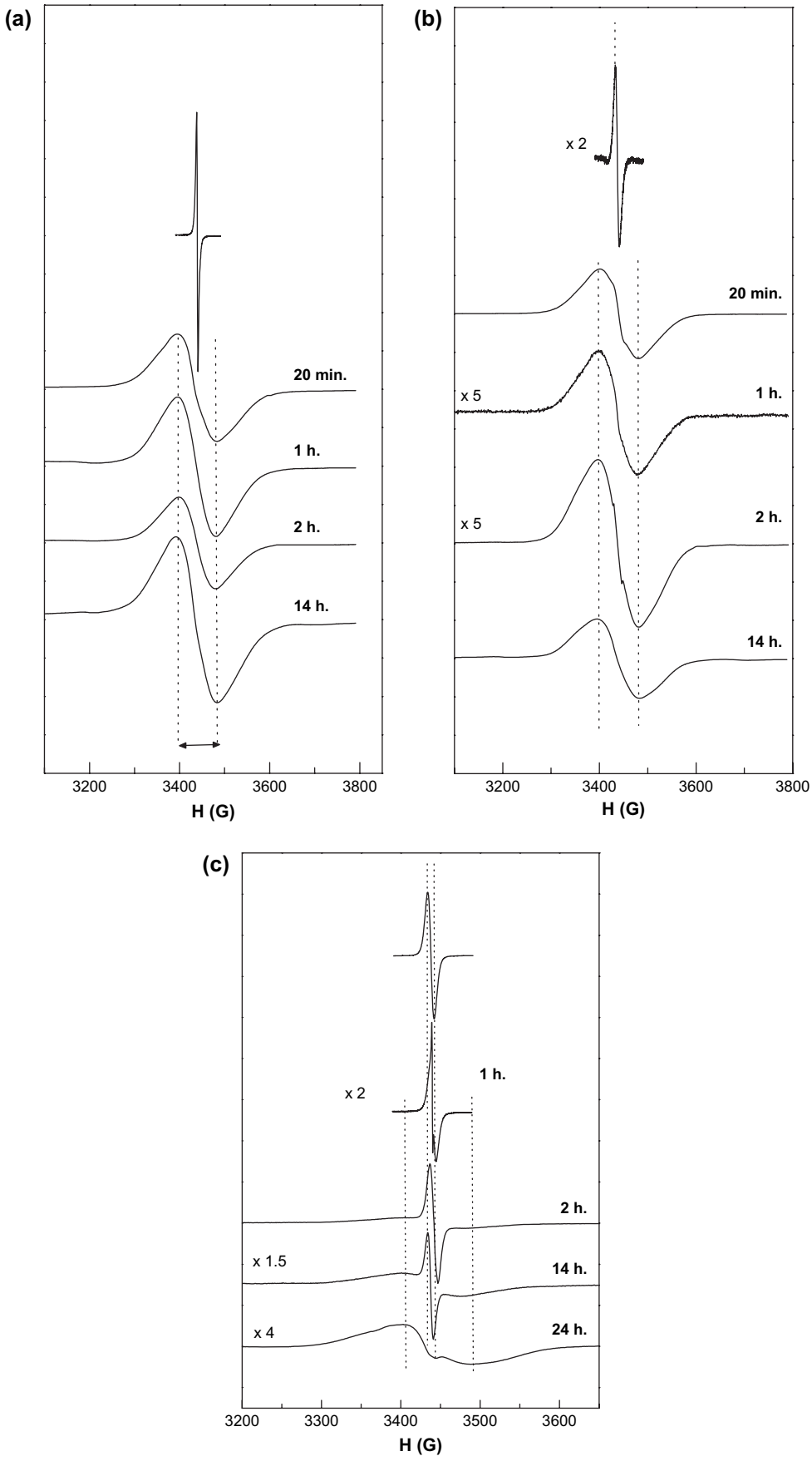

Fig. 7. EPR spectra of the virgin polymer and of the fluorinated samples for various durations: Kovacic PPP_K (a), Polysciences PPP (b) and Polysciences PPP post-treated (c).

3.2.3. Electron paramagnetic resonance study

The EPR response of PPP (Fig. 7a and b) is attributed according to several hypotheses [14]: (i) some of the catalyst formed during the synthesis are buried into the polymer bulk; (ii) twisting of the polymer chains renders these radical species inaccessible; (iii) polynuclear structure, *i.e.* cross-linking, supporting dangling bonds can be also formed during the synthesis and the thermal treatment. The EPR spectra recorded at room temperature change significantly after the fluorination whatever its duration. Only the Landé factor g remains constant, close to 2.0030 ± 0.0005. This value is typical of free radicals and/or localized structural defects. In the cases of PPP_K and PPP_P (Fig. 7a and b, respectively), after the treatment under fluorine gas at room temperature, a very important widening of the signal is observed, the peak-to-peak linewidth (ΔHpp) increases from 3.0 and 7.8 G for the PPP_K and PPP_P, respectively, to approximately 80 G. The origin of this broad signal is identified as carbon dangling bonds (DB) having a localized spin. Dangling bonds are structural defects corresponding to π-radicals generally formed during bond cleavage. This type of radicals is localized and very unstable but, when trapping into the carbonaceous bulk, it can exist with long-life as in our case. Such spin carriers have already been proposed for fluorinated graphites [25] and in fluorinated amorphous carbons' thin films. Contrary to the narrow line of the starting PPP, the broad signal cannot be simulated by a pure Lorentzian or Gaussian profile. This profile could result from a non-solved super-hyperfine structure (SHFS) of the dangling bond electrons interacting with the neighboring fluorine nuclei (nuclear spin number for ^{19}F: $I = 1/2$). For PPP_K and PPP_P, due to their reactivity with F_2, as soon as the first step of fluorination, the initial connection defects disappear and long-life DB are then formed. The EPR spectra were insensitive to the duration of the exposition to air atmosphere.

The behavior of PPP_T-T250 is different (Fig. 7c), after the treatment for 2 h, the initial narrow line is preserved. An additional narrow signal (ΔHpp = 1.1 G) is present, corresponding to an intermediate compound. The broad signal of DB appears after 2 h treatment with F_2. The narrow signal of pristine PPP is also present on this spectrum, because a part of the virgin PPP_P-T250 did not react with fluorine. These results corroborate the other characterizations about the compared reactivity of the PPPs.

The spin density of the DB was investigated for the various polymers (Fig. 8). For PPP_K and PPP_P, the fluorination for 20 min results in a significant increase in the spin density (*e.g.* from 0.8×10^{18} to 57.0×10^{18} spins g^{-1} for Kovacic PPP). The formed DB are then partially eliminated by reaction with F_2 when the treatment duration is increased except for the longest duration for which Ds increases in the both cases. Once again, a different behavior is observed for PPP_P-T250 since Ds continuously increases with the fluorination duration.

4. Discussion

The characterization of the fluorinated polymers obtained starting from different PPPs has shown that the reactivity of

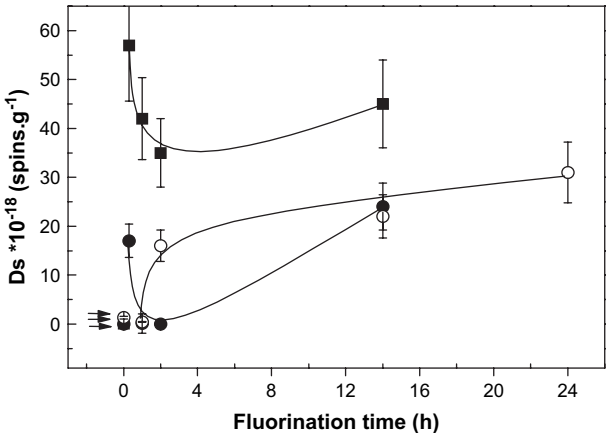

Fig. 8. Evolution of the spin density upon fluorination for the various starting materials: (■) PPP_K, (●) PPP_P and (○) PPP_P-T250.

the Kovacic PPP is higher than that for the other two Polysciences PPP, raw and heat treated, and that the aromaticity is lost upon the direct fluorination and a few phenyl rings are broken forming CF_2CF_3 side chains as by-products. A reaction mechanism can be proposed in which residual hydrogen atoms are still present (Eq. (1)) contrary to the perfluorination:

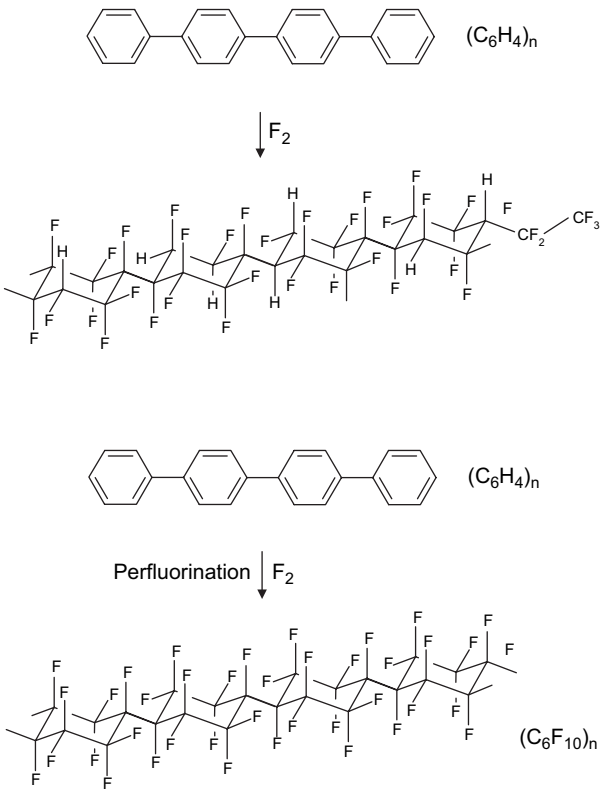

For a better understanding of such difference in reactivity with respect to F_2 gas, further investigation must be carried out and various parameters can be involved. We focus on two factors which appear paramount at two different scales: (i) macroscopic, namely morphology and granulometry of the powder; (ii) molecular, *i.e.* crystallinity and chain length. The heat treatment of PPP_K (annealing) allows the crystallinity to be increased from 23 to 30% and the chain length to change from

11–12 to 15–16 phenyls per chain. This latter value was estimated according the procedures described in Refs. [26] and [14,27]. The crystallinity was estimated by two methods, *i.e.* Ruland [28] and Hermans methods [29]. Moreover, the increase in the density and in the coherence lengths along the *a* and *c* axes reveals that an ordering of the polymer occurs during the annealing, simultaneously to the decrease of the catalytic residues (Cl, Cu, Al) and the hydrogen content, which is mainly explained by the increase of the cross-linking amounts (Table 4). As a matter of fact, EPR characterization reveals an increase of the spin density after the annealing. Cross-linking is described as a probable origin of the EPR signal for Kovacic PPP [16]. Catalyst residues (Cu, Al, Cl) are progressively removed during the annealing. A decrease in the reactivity of PPP_K with F_2 after annealing (Fig. 1 and Table 1) can thus be explained by a better structural organization which could limit the diffusion of fluorine, and also by an increase in the stability of the polymer due to the greater π-delocalization.

The powder morphology must also be taken into account. The SEM images of PPP_K before and after annealing are displayed in Fig. 9. Both the granulometry and the shape of the powders are sensitive to the annealing. Wherever into the raw polymer, the grains exhibit disordered forms whereas they are more organized as plates and rods after the annealing (Fig. 9c and d). These rods and plates of a few tens of micrometers (60–100 μm) are made up of fibrils packed in globular structure as suggested by Froyer [30], and later by Pradere [31].

Regarding the SEM images (Fig. 9e and f), the surface properties of the as-synthesized and annealed powders are close in agreement with B.E.T. measurements of 55 and 80 $m^2\,g^{-1}$ for the PPP_K and PPP_K-T400, respectively. As proposed by Zolotova and Volfkovich [32], the porous structure of PPP, annealed or not, exhibits a double dispersion of the pores: (i) small pores (diameter lower than 2.5 nm), which are probably due to the space between the chains; (ii) broader pores (between 80 and 2000 nm) due to the tangled fibrils. This duality appears on the SEM images of the two polymers (Fig. 9e and f).

The SEM images qualitatively reveal an increase of the grain size explaining the lower reactivity of annealed PPP in comparison with the raw polymer. Then, macroscopic (granulometry) and molecular effects (chain length and crystallinity) combine to induce a consequent decrease in the reactivity after annealing.

In the following part, these parameters are checked to explain the differences between the polymers issued from the Kovacic's synthesis and provided by Polysciences.

Firstly, the chemical compositions must be remembered: $C_6H_{3.85}$ for PPP_K and $C_6H_{2.88}$ for PPP_P resulting from different connection modes. The presence of the oligomers into PPP_P is prejudicial since, in addition to the reaction with the polymer chain, fluorine can react in a preferential way with the oligomers. Moreover, the estimation of the chain length is no more possible due to these oligomers. Nevertheless, Kovacic and Jones [14] have compared the various syntheses of PPP and concluded that the Kovacic method provides the longest chain (longer than 12 phenyls per chain). Polysciences PPP exhibits shorter chains, and in addition, the presence of oligomers. Considering this parameter, a higher reactivity is expected for PPP_P in comparison to PPP_K, but the opposite behavior is experimentally observed. So, another dominant parameter must be considered. The granulometry of the two studied polymers is very different (Fig. 10); the average size of the grains for the Kovacic PPP is lower with an average diameter of 66.8 μm and a broad diameter distribution ranging between 3.6 and 145.0 μm. The average diameter for PPP_P is 271.9 μm and the distribution is between 5.0 and 560.0 μm. For solid–gas reaction, the lower the granulometry is, the higher the reactivity is. The finest granulometry facilitates the reaction of the fluorine gas with the powder and thus enhances the reactivity. The macroscopic effect overrides the effect of the chain length and explains the higher reactivity of PPP_K when compared to PPP_P.

In the case of Polysciences PPP, the thermal treatment at 250 °C eliminates the oligomers but results also in a partial pyrolysis with both reorganization and a reduction in the H/C molar ratio. Consequently, the morphological and chain length effects cannot be taken into account to explain the lowest reactivity of PPP_T with F_2. This sample exhibits similarities with disordered hydrogenated carbons. The reactivity with fluorine of such disordered matrix is already known and is significantly lower than that of PPP [33].

Table 4
Comparison of the as-synthesized and annealed PPP_K

Kovacic PPP	As-synthesized	Annealed
Composition (chemical analysis) % w/w	$C_6H_{3.85}$	$C_6H_{3.81}$
C	92.2	93.0
H	4.9	4.9
O	0.4	0.3
Cl	1.1	0.5
Al	0.4	0.3
Cu	0.1	<0.1
Crystallinity (%, ±2)	23 (Ruland [28]); 25 (Hermans [29])	30 (Ruland [28]); 32 (Hermans [29])
Coherence lengths (nm) along the *a* and *c* axes (L_a and L_c, respectively)[a] (±1 nm)	$L_a = 5.4$; $L_c = 5.5$	$L_a = 7.0$; $L_c = 7.0$
Density[b]	1.36	1.38
Chain length (phenyl rings per chain)[c]	11–12	15–16
B.E.T. surface ($m^2\,g^{-1}$)	55	80

[a] Estimated by the Scherrer formula $L = 0.9^*\lambda/\Delta 2\theta^*\cos\theta$ where $\lambda = 0.15406$ nm (Cu(Kα)), θ and $\Delta\theta$ are the diffraction angle and the full width at half maximum of the diffraction peak.
[b] Obtained by helium pycnometry.
[c] Estimated from NMR [14,27] and IR data [13,26].

5. Conclusion

Thanks to a physicochemical characterization performed mainly by ^{13}C and ^{19}F NMR, FT-IR and EPR, the reactivity of various poly(*p*-phenylene) with fluorine gas was underlined as a function of both the polymer synthesis and the thermal post-treatment. The fluorination mechanisms were established in each case. Whatever the sample, the aromatic character is lost forming $>CF_2$ groups. A few phenyl rings

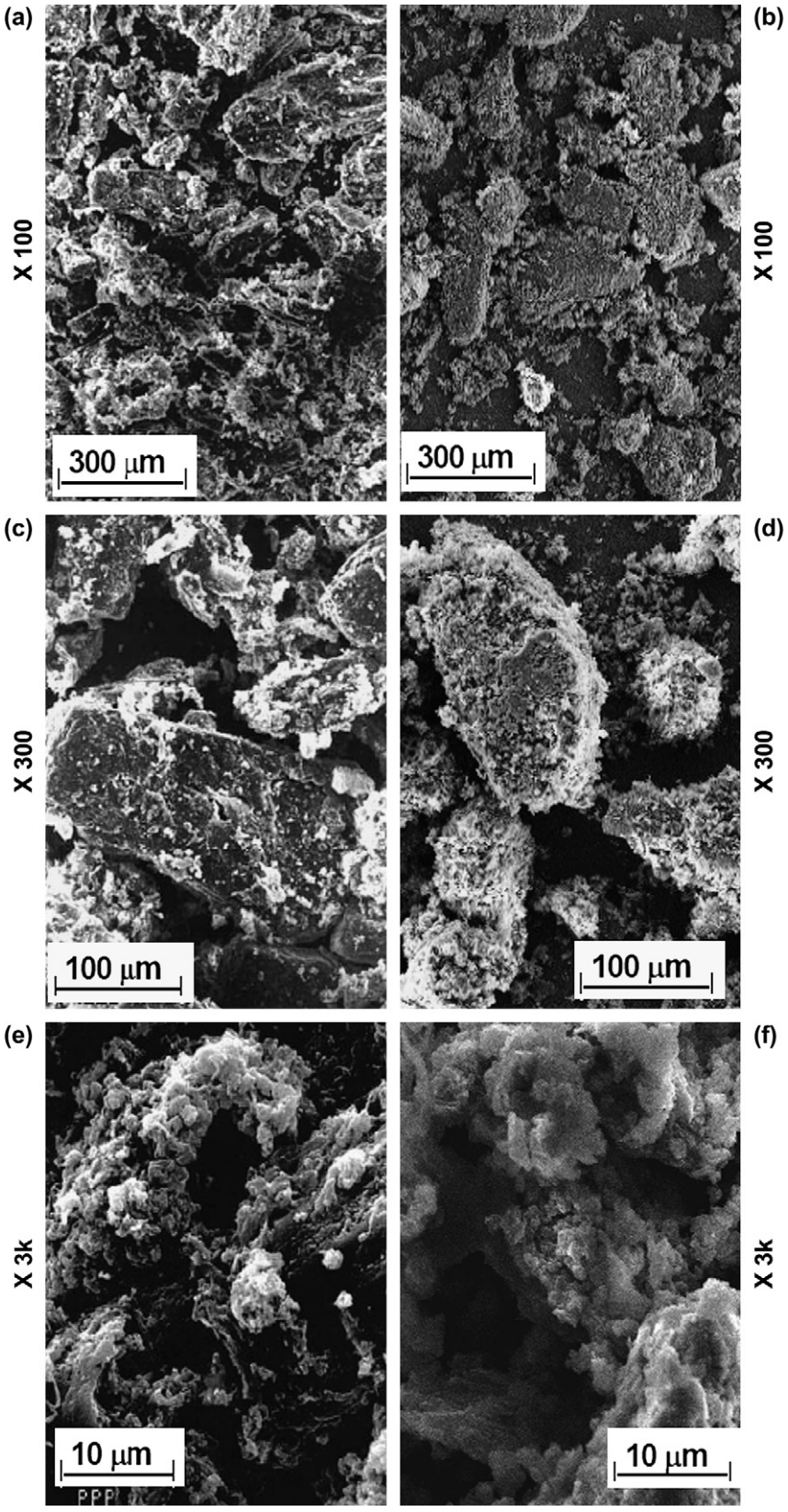

Fig. 9. SEM images at various scales of Kovacic PPP, as-synthesized (a, c, e) and annealed (b, d, f).

are broken resulting in CF_2CF_3 side chains as by-products. So, reactivity with fluorine gas of poly(*p*-phenylene), a conjugated polymer, was investigated by taking into account morphological and molecular effects. In order to change the granulometry, the surface properties, and the physicochemical properties, *i.e.* the chain length and the crystallinity, of two

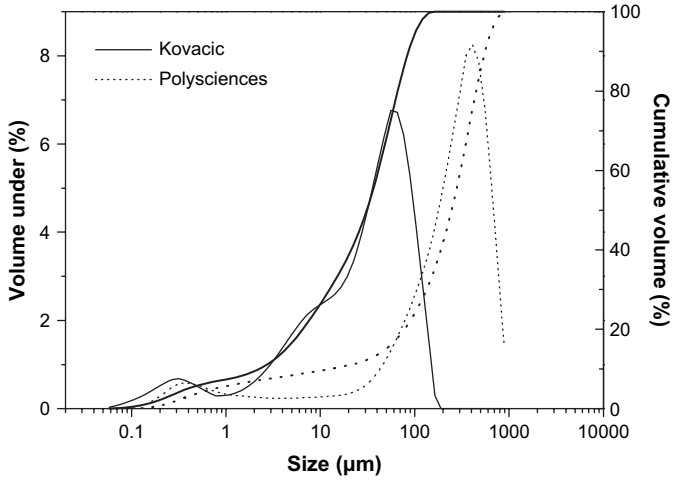

Fig. 10. Particle-size distribution of PPP samples (Kovacic and Polysciences) and corresponding integral curves.

polymers issued from the conventional Kovacic's synthesis and a commercial product (Polysciences) were studied as well as the compounds obtained after a thermal treatment of these two polymers. All these parameters influence the reaction of PPP with F_2. In the case of Kovacic PPP, the thermal treatment, similar to an annealing, improves the chain order by increasing the chain length and the crystallinity and results in the structuration of the powder grains as large plates and rods. By comparing raw and annealed polymers, the higher reactivity was observed when the powder exhibits smaller grains, shorter chain length and lower crystallinity (as-synthesized Kovacic PPP). Polysciences PPP contains residual oligomers and an attempt to remove these residues by a thermal treatment under vacuum was unsuccessful because it results in the conversion of the polymer into disordered hydrogenated carbons, which are similar to a pyrolyzed polymer. So, the reactivity of this resulting material is significantly decreased in comparison with the pristine polymer. Finally, morphological effects, rather than the chain length, explain the lower reactivity of Polysciences PPP when compared to Kovacic polymer since the grain size is substantially higher for the commercial product.

Acknowledgement

The authors would like to thank Dr. Jean-Marie NEDELEC (Laboratoire des Matériaux Inorganique UMR6002) for the N_2 sorption and laser granulometry measurements.

References

[1] Kharitonov AP, Taege R, Ferrier G, Teplyakov VV, Syrtsova DA, Koops GH. J Fluorine Chem 2005;126(2):251–63.
[2] Jeremy J, Hillmyer MA. Prog Polym Sci 2002;27(5):971–1005.
[3] Kharitonov AP, Moskvin YL, Syrtsova DA, Starov VM, Teplyakov VV. J Appl Polym Sci 2004;92(1):6–17.
[4] David A. Polym Rev 2006;46(3):315–27.
[5] Takasaki T, Kuwana Y, Takahashi T, Hayashida S. J Polym Sci Part A Polym Chem 2000;38:4832–8.
[6] Dubois M, Guérin K, Giraudet J, Pilichowski JF, Thomas P, Delbé K, et al. Polymer 2005;46:6736–45.
[7] Hayes LJ, Dixon DD. J Fluorine Chem 1977;10(1):17–26.
[8] Hewes JD, Curran S, Leone EA. J Appl Polym Sci 1994;53(3):291–5.
[9] Lagow RJ, Wei HC. Fluoropolymers 1999;1:209–21.
[10] Yamamoto T, Bundo M, Yamamoto A. Chem Lett 1977;7:833–4.
[11] Chaturvedi V, Tanaka S, Kaeriyama K. Macromolecules 1993;26(10):2607–11.
[12] Taylor SK, Bennet SG, Khoury I, Kovacic P. J Polym Sci Polym Lett Ed 1981;19(2):85–7.
[13] Kovacic P, Oziomek J. J Org Chem 1964;29(1):100–4.
[14] Kovacic P, Jones MB. Chem Rev 1987;87(2):357–79.
[15] Froyer G, Maurice F, Goblot JY, Fauvarque JF, Petit MA, Digua A. Mol Cryst Liq Cryst 1985;118(1–4):267–72.
[16] Dubois M. Thesis, Université Nancy I; 1999.
[17] Brown CE, Jones MB, Kovacic P. J Polym Sci 1980;18:653–8.
[18] Legeay G, Coudreuse A, Legeais J-M, Lerner L, Bulou A, Buzaré J-Y, et al. Eur Polym J 1998;34(10):1457–65.
[19] Fischer D, Lappan U, Hopfe I, Eichhorn K-J, Lunkwitz K. Polymer 1998;39(3):573–82.
[20] Dubois M, Naji A, Buisson JP, Humbert B, Grivei E, Billaud D. Carbon 2000;38:1411–7.
[21] Miller JB, Dybowski C. Synth Met 1983;6:65–8.
[22] Watanabe N, Nakajima T, Touhara H. Graphite fluorides. Amsterdam: Elsevier; 1988.
[23] Panich AM. Synth Met 1999;100(2):169–85.
[24] Krawietz TR, Haw JF. Chem Commun 1998;19:2151–2.
[25] Dubois M, Guérin K, Pinheiro JP, Masin F, Fawal Z, Hamwi A. Carbon 2004;42(10):1931–40.
[26] Aeiyach S, Lacaze PC. J Polym Sci Part A Polym Chem 1989;27(2):515–26.
[27] Barbarin F, Berthet G, Blanc JP, Fabre C, Germain J, Hamdi M, et al. Synth Met 1983;6:53–9.
[28] Ruland W. Acta Crystallogr 1961;14:1180.
[29] Hermans PH, Weidinger A. Macromol Chem 1961;24:44–6.
[30] Froyer G, Maurice F, Mercier JP, Rivière D, le Cun M, Auvray P. Polymer 1981;22:992–4.
[31] Boudet A, Pradere P. Synth Met 1984;9:491–4.
[32] Volfkovich Y, Bagotzky VS, Zolotova TK, Pisarevskaya EY. Electrochim Acta 1996;41:1905–12.
[33] Leroux F, Dubois M. J Mater Chem 2006;16:4510–20.